Article

A General Mathematical Formulation for Winding Layout Arrangement of Electrical Machines

Massimo Caruso [1] [ID] **, Antonino Oscar Di Tommaso** [1,*] [ID] **, Fabrizio Marignetti** [2] [ID] **, Rosario Miceli** [1] [ID] **and Giuseppe Ricco Galluzzo** [1] [ID]

[1] Department of Energy, Information Engineering and Mathematical Models (DEIM), University of Palermo, viale delle Scienze, Building nr. 9, 90128 Palermo, Italy; massimo.caruso16@unipa.it (M.C.); rosario.miceli@unipa.it (R.M.); giuseppe.riccogalluzzo@unipa.it (G.R.G.)

[2] Department of Electrical and Information Engineering (DIEI), University of Cassino and South Lazio, via G. Di Biasio, 43, 03043 Cassino, Italy; marignetti@unicas.it

[*] Correspondence: antoninooscar.ditommaso@unipa.it

Abstract: Winding design methods have been a subject of research for many years of the past century. Many methods have been developed, each one characterized by some advantages and drawbacks. Nowadays, the star of slots is the most widespread design tool for electrical machine windings. In this context, this paper presents a simple and effective procedure to determine the distribution of the slot EMFs over the phases and of the winding configuration in all possible typologies of electrical machines equipped with symmetrical windings. The result of this procedure gives a Winding Distribution Table (WDT), which can be used to define coils and coil groups connections and also to simply implement winding optimizations techniques, such as zone widening, imbrication, etc. Moreover, this procedure can be easily implemented on a computer in order to perform automated winding designs for rotating electrical machines. Several examples are provided in order to validate the proposed procedure.

Keywords: electrical machines; winding design; symmetrical winding; star of slots

1. Introduction

Over the last century, several procedures for the design of the windings of electrical machines have been proposed in the literature. The first studies on the synthesis of windings date back to the first decade of the 20th century and can be attributed to E. Arnold, R. Richter and W. Kauders. The first proposed a systematic method based on the so-called star of slots (the original German term was *Nutenstern*) to solve design issues on windings of both AC and DC machines [1,2], whereas the second author improved these techniques particularly for AC machines [3]. In the same period W. Kauders, who changed his name in W. Klima after 1945, developed a study of two and three-phase windings, also providing general formulas to determine the winding factors [4,5]. In the 1950's Richter completed his researches and published a book concerning this topic [6]. Thus, it can be stated that a wide part of the literature regarding the winding design was accomplished in Europe mainly by German researchers from late 1890 to early 1960's and many of these works were collected in a three-volumes book, written by the Austrian H. Sequenz [7–9]. In the same time, French researchers, such as H. de Pistoye [10], followed by German-Czechoslovakians [5,11], Italians [12], Japanese [13] and American scholars, as M. Liwschitz-Garik, Malti-Herzog, Hellmund and E. M. Tingley [14–19], also contributed to the significant development of this area, but limiting their method to solve single, two and three phase windings. Other interesting manual and/or automated methods and algorithms were developed later [20–24]. Each of these methods can be used for specific design constrains and none can be considered as universally valid. This is mainly due to the fact that, during the first seven

decades of the 20th century, researchers focused only on DC machines and single-phase, two-phase and three-phase AC machines. Nowadays, the interest is also directed towards multiphase machines, particularly with five, six, seven phases and more [21,22,25–27]. Today, the star of slots seems to be the most widespread design tool for electrical machine windings [23,28–31].

The cited winding design methods provide relevant drawbacks and difficulties if they are applied for these new winding configurations. For instance, Tingley's method, which is also based on the evaluation of numeric tables, has been developed only for two and three phase windings; multi-phase windings are limited only to odd number of phases and some combinations of slots, poles and phases cannot be solved [7,9,17]. In [17] it is possible to find the first attempt to treat multi-phase windings, including "dead-coil" windings. Unfortunately, Malti and Herzog developed a rather complex method, also based on the use of tables, requiring the distinction of at least 4 types of winding and the construction of the same amount of tables. Moreover, this treatise covers only non-reduced multi-phase systems, omitting reduced ones, which, in truth, had not significant importance at that time. Anyway, none of these methods seems to be suitable to implement winding optimization techniques. Another interesting winding design method, based on tables, has been proposed by P. Wach, but it does not seem to be suitable for implementation of interspersing techniques [24,32].

In this context, we propose a simple, powerful and general procedure, that can also be considered as an alternative to the method based on the star of slots, suitable for all symmetrical winding configurations, covering also concentrated topologies and even reduced or normal (radial symmetrical) systems [22,33]. Indeed, a hint of a similar method was fleetingly introduced by F. Heiles in [34]; however, he never developed it and later researchers, unexpectedly, did not give it an adequate consideration. The proposed method, namely WDT (Winding Distribution Table), allows the design of all *m*-phase single or double-layer windings (including overlapping and non-overlapping ones), providing fast and automated winding designs. Moreover, by manipulating the WDT with simple procedures, it is possible to implement optimization techniques, such as: chording (coil pitch shortening), zone widening (coil side shift in a slot), interspersing (i.e., transfer of one or more coils to another zone [33]) (or imbrication) [3,6,9,20,35,36] and double chording [16] (consisting on the adoption of both chording and interspersing [9,20]). These optimization techniques can be used to decrease significantly one or more undesired winding factor harmonics, improving, therefore, the harmonic content of both the air-gap magneto-motive force (MMF) and the phase electro-motive forces (EMFs). The procedure for the determination of the WDT and its use are hereafter presented and, in order to validate this procedure, the comparison with the traditional star of slots method is carried out with the help of several examples, highlighting how the latter be more complex to construct because of several geometrical issues.

More in detail, this paper is structured as follows: the general conditions allowing the definition of the winding configuration are described in Section 2, the proposed WDT procedure is described in detail in Section 3 and the validation of the procedure through the description of several examples of symmetrical windings is provided in Section 4.

2. Symmetry Conditions for Winding Design

The symmetry conditions are valid both for non-reduced and normal systems, for which the mutual phase displacement is $\alpha_{ph} = 2\pi/m = 360°/m$, as well as for reduced system for which the mutual phase displacement is $\alpha_{ph} = \pi/m = 180°/m$. For an electrical machine with N slots, m phases, n_{lay} layers and p pole pairs, the winding symmetry can be evaluated by using the factors n_{wc}, namely the number of wound coils per phase, and the number of coils having different phases g, which are defined, respectively, as

$$n_{wc} = n_{lay}\frac{N - n_{es}}{2m} \tag{1}$$

$$g = \begin{cases} \frac{n_{lay}N}{2mt} & \text{for normal and non−reduced systems} \\ \frac{N}{2mt} & \text{for reduced systems,} \end{cases} \tag{2}$$

as defined in Table 2.4, page 98 of [27,33]). where n_{es} represents the number of empty slots (dead-coil winding) in the case of single layer windings, and the number of unwound coils, in case of double layer windings and:

$$t = \gcd(N, p), \tag{3}$$

is the greatest common divider between N and p, whereas $n_{lay} = 1, 2$ is the number of layers.

The winding symmetry is assessed with the help of the following conditions:

$$\begin{cases} n_{wc} \in \mathbb{N} & \text{for coil windings} \\ n_{wc} \in \{\mathbb{N}, \mathbb{N}/2\} & \text{for bar windings}, \end{cases} \tag{4}$$

and

$$\begin{cases} g \in \mathbb{N} & \text{for symmetrical windings} \\ g \notin \mathbb{N} & \text{for unsymmetrical windings}, \end{cases} \tag{5}$$

where $\mathbb{N}$ is the set of natural numbers. Bar windings can be defined as windings composed by coils having only one turn and whose active coil sides are composed by bars (e.g., Roebel bars).

If conditions (4) and the first of Equation (5) are satisfied, the winding is symmetrical; otherwise, it is asymmetrical. In any case, for the computation of (1), the initial value of the empty slots n_{es} is assigned equal to zero. If (4) is not satisfied, then the value of n_{es} must be determined through formula

$$n_{es} = N - \frac{2 \cdot m \cdot \lfloor n_{wc} \rfloor}{n_{lay}}, \tag{6}$$

where $\lfloor n_{wc} \rfloor$ is the largest integer less than or equal to n_{wc}. In this way, considering empty slots or unwound coils, the first condition of winding symmetry expressed by (4) is always satisfied. It must be underlined that (6) is valid only if $m > 1$.

The assignment of n_{es} between the different phases can be arbitrary if $n_{es} \neq m$ (even if the distribution of the empty slots should be as uniform as possible among the phase sections). If $n_{es} = m$, the empty slots should be chosen one for each phase (uniformly distributed), so that the corresponding slot EMF phasors are phase-shifted by $2\pi/m = 360°/m$ in case of normal systems and by $\pi/m = 180°/m$ in case of reduced systems.

An exception is valid if $m = 1$ (single phase windings), for which the following equation has to be considered in place of (6):

$$n_{es} = \left\lfloor \frac{N}{3} \right\rfloor, \tag{7}$$

where a winding covering 2/3 of the slots is considered.

The number of wound slots per pole per phase is determined as

$$q = \frac{N - n_{es}}{2p \cdot m} = \frac{n_{wc}}{n_{lay} \cdot p} = a + \frac{z}{n_{lay} \cdot p}, \tag{8}$$

where $a = \lfloor q \rfloor$ and $z/n_{lay} \cdot p$ is a proper fraction. If q is an integer number, then the winding is called "integral slot winding". Otherwise, if q is a fractional number, the winding is defined as "fractional slot winding".

Moreover, in the cases where $n_{es} > 0$, it is advantageous to define the number of slots per pole per phase given by

$$Q = \frac{N}{2p \cdot m} = \frac{n_{wc}}{n_{lay} \cdot p} + \frac{n_{es}}{2p \cdot m} = q + \frac{n_{es}}{2p \cdot m}. \tag{9}$$

If $n_{es} = 0$, then $Q = q$.

In order to recognize basic winding configurations when q is a fractional number and $n_{es} = 0$, the following equation must be taken into account (considering (8)):

$$z = n_{lay} \cdot p \cdot (q - a) = n_{wc} - n_{lay} \cdot p \cdot a, \tag{10}$$

which gives the numerator of the proper fraction contained in (8). In this equation the case $n_{lay} = 2$ can be referred both to double-layer windings and to single-layer bar windings when $n_{wc} \in \mathbb{N}/2$. In the last case, with $n_{es} = 0$, $n_{lay} = 1$ and $k \in \mathbb{N}$, relation (1) becomes

$$n_{wc} = \frac{k}{2} = \frac{N}{2m},$$

or

$$\frac{N}{m} = k \in \mathbb{N},$$

which meets condition (1) for double layer windings. Furthermore, the factor t' must be defined for fractional slot windings:

$$t' = \gcd(z, p). \tag{11}$$

If $t' = 1$, the winding is a basic one. Otherwise, the winding is composed by t' repetitions of the same basic winding, which is composed by $N' = N/t'$ slots and $p' = p/t'$ pole pairs. If $n_{es} > 0$ then it is sometimes convenient to set $t' = 1$ in order to avoid the case $n_{es} > m$ (a case in which there would be too much unwound slots or coils).

For integer slot windings ($q \in \mathbb{N}$ and $n_{es} = 0$) the number of repetitions is equal to $t' = p$, because N and p have the same divisor equal to p itself as can be deduced by (8).

3. WDT Procedure

The proposed winding distribution procedure is based on the construction of a Winding Distribution Table (WDT), which allows the assignment of a specific stator slot to a winding phase section [6,23]. WDT is a winding diagram representation in table form that can be used in a design tool. In this table each row corresponds to a phase (m) and number of columns equals to slots per phase (N/m). This matrix is filled row by row starting from slot nr. 1 and leaving $N/m \times p$ cells (as phasor pair or group) before the slot nr. 2 is populated to the matrix. Hereafter the basic rules to determine the WDT are defined.

3.1. Determination of WDT

This table, containing N elements, is composed by a number of rows equal to m and a number of columns equal to

$$n_c = \frac{N}{m}, \tag{12}$$

whose elements are ordered as shown in Table 1.

Table 1. Order of the WDT elements.

	col. 1	col. 2	...	col. n_c
row 1	1	2	...	n_c
row 2	$n_c + 1$	$n_c + 2$	...	$2n_c$
row 3	$2n_c + 1$	$2n_c + 2$	...	$3n_c$
$\vdots$	$\vdots$	$\vdots$	$\ddots$	$\vdots$
row m	$(m-1)n_c + 1$	$(m-1)n_c + 2$	...	mn_c

In the case of a single-layer winding, the WDT elements are referred to phasors associated to each slot or, in other words, to each coil side: a single-layer machine winding is composed by

$N = 2m \cdot n_{wc}$ coils. In the double-layer winding configuration, the WDT elements are referred to a coil side, whereas the second coil side is defined by the coil pitch y_c usually expressed in terms of number of slots. In this case, the machine winding is composed by $N = m \cdot n_{wc}$ coils.

The definition of the WDT starts by assigning the slot number 1 to the first cell of Table 1. Then, the slot number 2 is assigned to the cell whose distance is equal to p cells from the first one, the slot number 3 to the cell whose distance is equal to p cells from the second one, following the orientation of the progressive numbering of the cells of Table 1. After N/p (if $N/p \in \mathbb{N}$) assignments, the procedure continues by imagining that the last cell of the table is ideally consecutive to the first: therefore, once the N-th table element is counted, the counting continues restarting from the first cell of the table. If the count ends in a filled cell, the adjacent empty cell will be filled with the counted slot. The procedure continues until the table is completely filled by the slot numbers.

In order to clarify this procedure, Table 2 reports the WDT referred to a simple integral slot symmetrical winding with $N = 24$, $p = 2$, $m = 3$ and $q = 2$. The Table is filled in $p = 2$ filling cycles, each one corresponding to $N/p = 12$ assignments. In fact, by starting from placing slot nr. 1 in the first cell (row 1, col. 1), the slot nr. 2 is placed after $p = 2$ cells (row 1, col. 3), till slot nr. 12 is assigned to the 23-th cell (row 3, col. 7), which corresponds to the N/p-th assignment and the first filling cycle is completed. The second cycle starts by counting p elements from cell nr. 23, which corresponds to element nr. 25. However, due to the periodicity of this winding configuration ($N = 24$), the element nr. 25 corresponds to the first element. Therefore, the slot nr. 13 will be placed in the adjacent empty second cell (row 1, col. 2). The vertical double bar separates the active conductors with positive EMF from those with negative EMF. In symmetrical windings, the double bar should be located around the middle of the table in order to gain the highest EMF. The star of slots corresponding to this configuration is plotted in Figure 1. The positive EMFs are reported in a thicker width with respect to the negative ones. It can be noticed, by comparing the rows of Table 2 with Figure 1, that the WDT is the tabular and linear representation of the star of slots, therefore there is virtually no need to use the star of slots. Anyway, hereinafter the stars of slots will be represented only for more clarity.

Table 2. Winding Distribution Table for a winding with $N = 24$, $p = 2$ and $m = 3$.

1	13	2	14	3	15	4	16
5	17	6	18	7	19	8	20
9	21	10	22	11	23	12	24

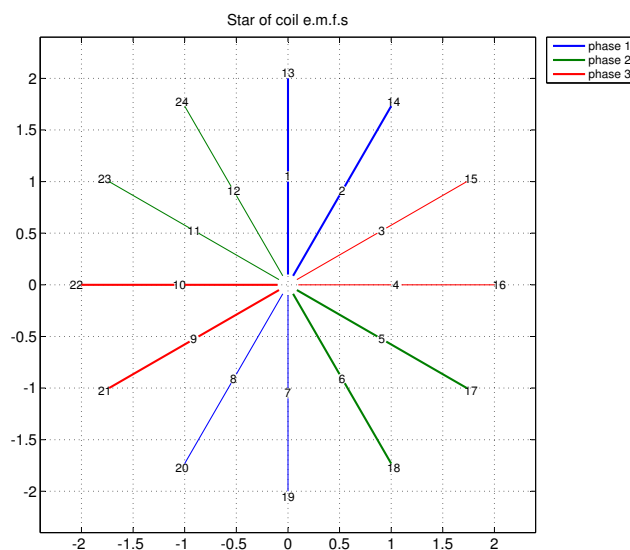(phase 1: blue, phase 2: green, phase 3: red).

Figure 1. Plot of the EMF star for a symmetrical winding with $N = 24$, $m = 3$ and $p = 2$.

Furthermore, it has been found that the WDT facilitates the practical arrangement for assembling the coils and form the final winding configuration. Indeed, the WDT contains information about which of the slots belong to each phase section. In fact, once the WDT has been created and the phases are defined for each slot, the end winding can be chosen in order to reduce the connections length between positive and negative slots (coil sides) of the same phase. For this purpose, WDT can be directly used to represent in plane the active coil sides and to identify their phase by simply following the WDT rows, as shown in Figure 2a, where every slot is already characterized by its EMF phase color and by its sign, a positive (up arrow) or a negative (down arrow), depending on the sign of each WDT element. The end-connection can then be drawn as shown in Figure 2b–d depending on the particular needs of designers (low leakage inductances, shortest end-windings, number of groups or end-connection planes).
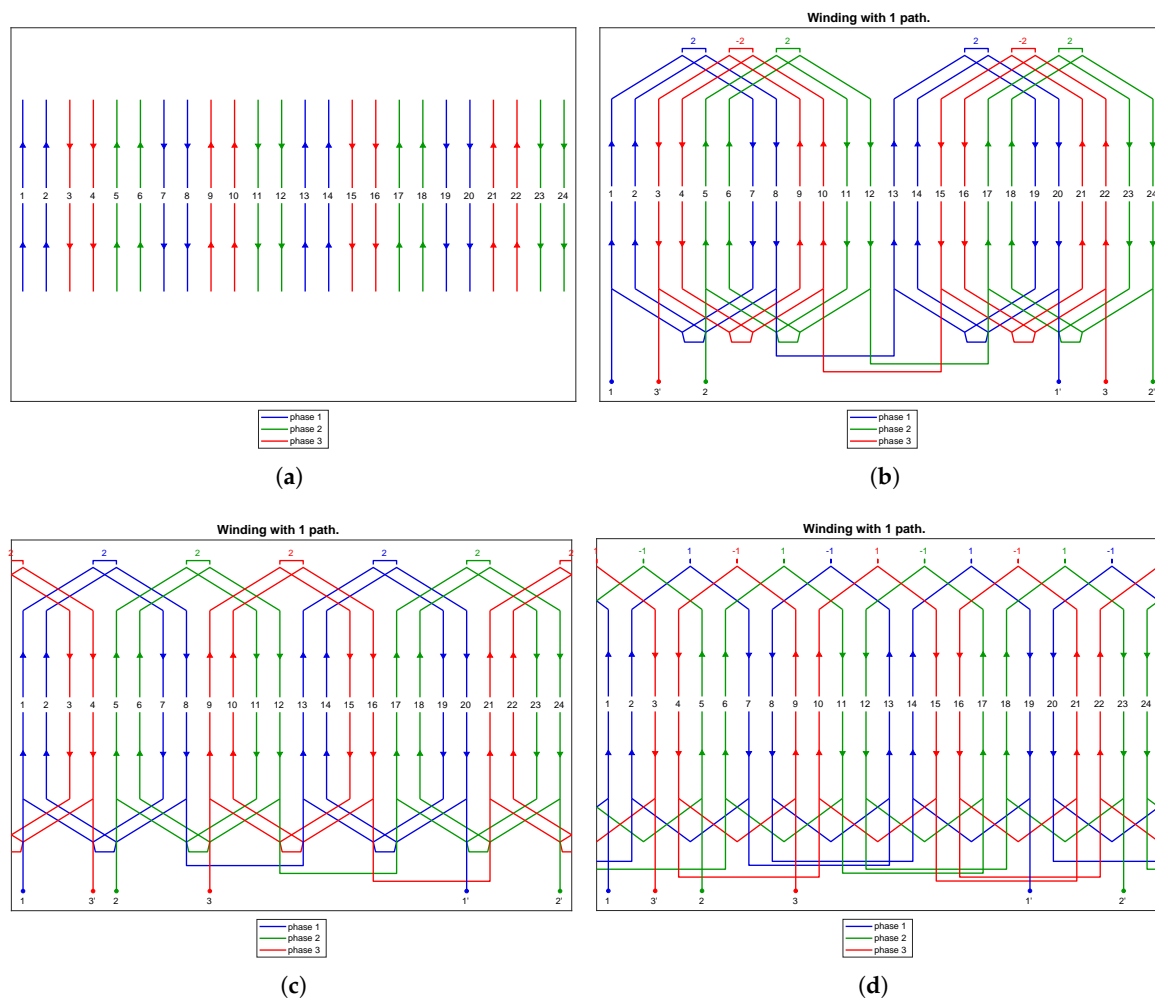

Figure 2. Winding schemes with different end winding layouts for a single-layer configuration with $N = 24$, $m = 3$, $p = 2$ and $q = 2$ derived from the WDT. (**a**) Without end connections; (**b**) for a split stator and three-plane end winding; (**c**) with two-plane end winding and (**d**) with three-plane end winding.

The parameter t given in (3) determines the number of superposing EMF stars related to the specific winding configuration. Therefore, in the WDT, the slots associated to the cells from $kt + 1$ to $(k + 1)t$ (with $k = 0, 1, 2, ..., N/t - 1$) will have the same phase-angle, by following the WDT path previously defined and shown in Table 2. In particular, each EMF star is composed by N/t phasors, phase-shifted to each other by an electrical angle α equal to

$$\alpha = t \cdot \frac{360°}{N}. \tag{13}$$

By following these considerations it is possible to reconfigure Table 1 and to build Table 3 as used in [3,6], in which the electrical angles φ_k of each slot-phasor pair are computed by the following formula:

$$\varphi_k = k \cdot \alpha \quad \text{with} \quad k = 0, 1, \ldots, N/t - 1. \tag{14}$$

With reference to the previous example, it can be noticed that each EMF star is composed by $N/t = 24/2 = 12$ phasors, phase-shifted to each other by an electrical angle α equal to

$$\alpha = t \cdot \frac{360°}{N} = 30°. \tag{15}$$

Therefore, $t = 2$ represents the number of phasors having equal phases. In this example (see Table 2), the pair of phasors 1–13, 2–14, 3–15, 4–16... have the same phase-shift. Moreover, the consecutive pairs are shifted between each other by an angle equal to 30°, as shown in Figure 1 (i.e., the pair 2–14 is phase-shifted by an angle of 30° with the pair 1–13). Thus, the phase-shifts of all phasors can be easily computed by considering Table 3. The resulting table is shown in Table 4.

Table 3. Electrical angles of the star of slots ($j = 1, ..., t$).

φ_k	0°	α	2α	$\cdots$	$(N/t - 1)\,\alpha$
1-st row	1	2	3	$\cdots$	N/t
$\vdots$	$\vdots$	$\vdots$	$\vdots$	$\ddots$	$\vdots$
t-th row	$(j-1)\,N/t + 1$	$(j-1)\,N/t + 2$	$(j-1)\,N/t + 3$	$\cdots$	N

Table 4. Electrical angles of the EMF star phasors for $N = 24$, $p = 2$ and $m = 3$.

Electr. Angles φ_k	0°	30°	60°	90°	120°	150°	180°	210°	240°	270°	300°	330°
Phasor pairs	1	2	3	4	5	6	7	8	9	10	11	12
	13	14	15	16	17	18	19	20	21	22	23	24

In truth, by considering that $q = 2$, the same WDT can be obtained considering the number of repetitions t' as defined by Formula (11). In fact, this winding can be seen as composed by $t' = 2$ repetitions of the same winding characterized by $N' = N/t' = 24/2 = 12$ slots, $m = 3$ phases and $p' = p/t' = 2/2 = 1$ pole pair ($n_{wc}' = n_{wc}/t' = 4$) and, therefore, the WDT can be seen as the composition of two basic WDTs as shown in Table 5. In this case the second WDT is created with the same rules above exposed but starting from slot $N/2 + 1$ till slot N. Now, by considering the two repetitions, this winding could be divided in two parallel connected branches. A comparison of Tables 2 and 5 shows their equivalence.

Table 5. Winding Distribution Table with $t' = 2$ repetitions, for a winding with $N = 24$, $p = 2$ and $m = 3$.

1	2	3	4		13	14	15	16
5	6	7	8	+	17	18	19	20
9	10	11	12		21	22	23	24

(phase 1: blue, phase 2: green, phase 3: red).

It will be demonstrated in the following sections that simple computations allow the determination of the winding distribution even for complex configurations.

3.2. WDT Post-Processing

After the WDT is created, the winding factors of the ν-th harmonic and the related proper phases for each $h-th$ phase can be computed through the following equations:

$$k_{wpv,h} = \frac{1}{2pqn_{lay}} \cdot \sqrt{\left(\sum_{n=1}^{2pqn_{lay}} C_{pv,h,n} \right)^2 + \left(\sum_{n=1}^{2pqn_{lay}} S_{pv,h,n} \right)^2} \tag{16}$$

and

$$\arg\left(k_{wpv,h} \right) = \text{atan2} \left(\sum_{n=1}^{2pqn_{lay}} S_{pv,h,n} \,,\, \sum_{n=1}^{2pqn_{lay}} C_{pv,h,n} \right), \tag{17}$$

where

$$C_{pv,h,n} = k \cdot \cos\left(2\pi pv \frac{|a_{h,n}|}{N} \right), \tag{18}$$

$$S_{pv,h,n} = k \cdot \sin\left(2\pi pv \frac{|a_{h,n}|}{N} \right), \tag{19}$$

$$k = \begin{cases} +1 & \text{if } a_{h,n} > 0 \\ -1 & \text{if } a_{h,n} < 0, \end{cases} \tag{20}$$

$a_{h,n}$ is a generic element of the WDT, $n = 1, 2, ..., N/m$ is the n-th column of the WDT and $h = 1...m$ is the h-th phase of the related winding. If the winding is symmetrical, the computation of harmonic winding factors can be limited to only one phase (for example the 1-st phase, i.e., $h = 1$). When dealing with double layer windings, also the negative coil sides (defined by their coil pitch y_c) have to be inserted in the WDT.

3.3. WDT for Symmetrical Non-Reduced and Normal Systems

In the case of radially symmetrical (radially symmetrical systems are defined as multiphase systems having a no-loaded neutral point [33]), otherwise called *normal* systems, in order to visualize, if required, all the positive and the negative phasors of the same phase in the same row, an adequate number of the last WDT columns (these group of columns are indicated in Figure 3 as "right side") must all be shifted in the upper direction by ζ shifts (see Figure 3) and their sign must be changed, where

$$\zeta = \begin{cases} \frac{m-1}{2} & \text{if } m \in \mathbb{U} \\ \frac{m}{2} - 1 & \text{if } m \in \mathbb{G}. \end{cases} \tag{21}$$

The number of columns to be shifted depends on the type of winding. In the case of a single layer symmetrical winding, $N/2m = n_{wc}$ columns must be shifted, due to the fact that the number of positive slots must be equal to the negative ones and the WDT will be divided into two equal left and right sides. In the case of a single layer bar winding, it may happens that n_{wc} be a fraction with the denominator equal to 2. Therefore, $n_{wc} \pm 1 = N/2m \pm 1$ columns should be shifted. For the double-layer configuration, this restriction is not necessary. Therefore, the number of positive and negative coils can be chosen properly, depending on the type of winding design optimization (maximization of the EMF, reduction of the harmonic content, simplicity of realization of end-windings, zone widening, etc.). In addition, in any case, a minus sign is added to the shifted columns, so that the coil sides with the negative EMF can be explicitly visualized within the WDT. It clearly appears that the groups of adjacent elements with the same sign located in each row of the WDT represent the winding zones of each phase. It should be noted that, in case of bar or double-layer windings, the number of columns

of the "left" and "right" side are, in general, given by $\lfloor N/m \rfloor$ and $\lceil N/m \rceil$, respectively, or *vice versa* (see Figure 3).
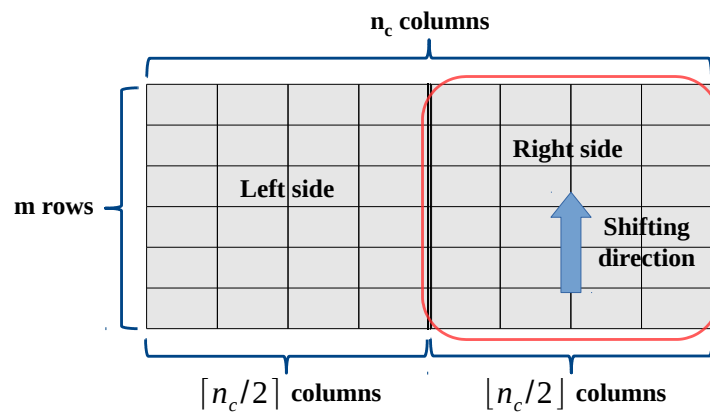

Figure 3. WDT for a generic normal system winding. The right side of WDT is shifted upwards by ζ steps.

3.4. WDT for Reduced Systems

For reduced systems the WDT is not affected by vertical shifting, but the quadrants named 1 and 3 in Figure 4 are simply swapped. In this case the WDT is valid for all windings with $m \in \mathbb{G}$ (for example in two-, four- or six-phase reduced system windings). The sign of the slot numbers in Quadrants 1 and 4 are then changed to account for negative coil sides. It should be noted that, in case of bar or double-layer windings, the number of columns of Quadrants 1 and 4 is, in general, given by $\lceil N/m \rceil$, whereas the number of columns of Quadrants 2 and 3 by $\lfloor N/m \rfloor$ or *vice versa*. After this operation the rows of the WDT should be reordered following the procedure of Table 6.
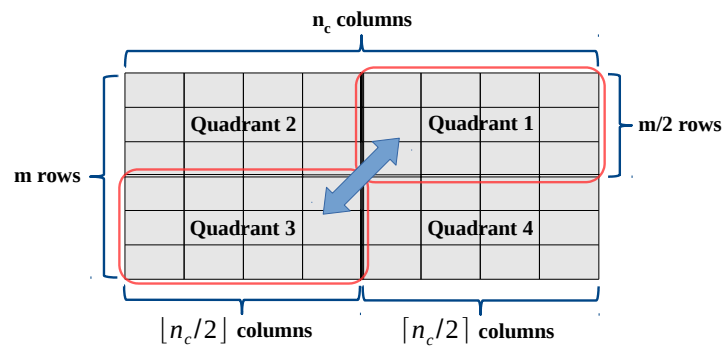
Figure 4. Swapping of the WDT quadrants in case of reduced systems and $m \in \mathbb{G}$.

Table 6. Reordering of the rows of a WDT for an m-phase reduced system winging with $m \in \mathbb{G}$.

Phases	col. 1	col. 1	...	col. n_c		Phases	col. 1	col. 1	...	col. n_c
1	...	...	...	...		1	...	...	...	...
$\vdots$	$\vdots$	$\vdots$	$\ddots$	...		$\frac{m}{2}+1$	...	...	...	...
						2	...	...	...	...
$\frac{m}{2}$	...	...	...	...	$\implies$	$\frac{m}{2}+2$	...	...	...	...
$\frac{m}{2}+1$	...	...	...	...		$\vdots$	$\vdots$	$\vdots$	$\ddots$	...
$\vdots$	$\vdots$	$\vdots$	$\ddots$	...		$\frac{m}{2}$	...	...	...	...
m	...	...	...	...		m	...	...	...	...

Reduced system whose number of phases is not a power of 2 are composed by m_g groups of m_u-phase systems shifted by an angle of

$$\alpha_g = \frac{\pi}{m} = \frac{180°}{m}, \tag{22}$$

where

$$m_u = \mathrm{gpf}(m), \tag{23}$$

is the greatest prime factor of m, and

$$m_g = \frac{m}{m_u}. \tag{24}$$

For example a reduced system winding with $m = 10$ phases can be decomposed into $m_g = 2$ groups of $m_u = 5$-phase systems; a reduced system winding with $m = 12$ phases can be decomposed into $m_g = 4$ groups of $m_u = 3$-phase systems. The even groups of a reduced system must then be multiplied by -1 in order to make them radially symmetrical, avoiding the use of a neutral line. Otherwise the sum of the resultant phase EMFs, that are all confined within an angle equal to π, would produce a non-zero value. The procedure will be cleared in Section 4.

3.5. WDT for Single-Phase Systems

For $m = 1$, the WDT is reduced to a single row composed by four sectors, as shown in Figure 5: the first sector is composed by $\lceil (N-n_{es})/2 \rceil$ cells, the second by $\lfloor n_{es}/2 \rfloor$ (or $\lceil n_{es}/2 \rceil$) cells (representing empty slots of the first unwound part), the third by $\lfloor (N-n_{es})/2 \rfloor$ cells and the last one by $\lceil n_{es}/2 \rceil$ (or $\lfloor n_{es}/2 \rfloor$) cells (representing empty slots of the second unwound part).
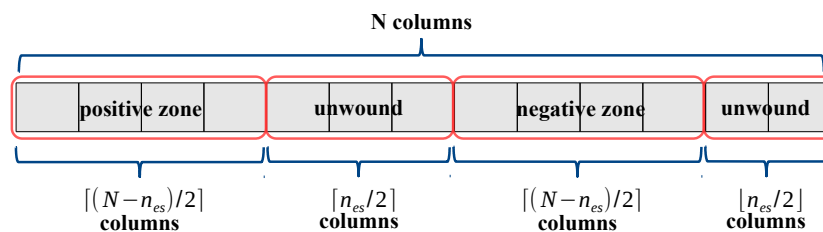

Figure 5. A possible WDT for single phase windings.

Another simple possible procedure to solve single phase windings is to consider them as derived from a three-phase winding, but excluding one phase (therefore, the "starting phase" can be located in the unwound slots). An example of this approach will be shown and discussed in the last example of Section 4.

4. Examples and Procedure Validation

In this Section several examples of winding configurations for electrical machines are reported in order to validate the proposed procedure. These examples can be adequate for the comprehension of the modality of construction of the WDT for each of the proposed electrical machine. Other more complex examples for multiphase windings are also considered and analyzed in the following subsections. The construction of the EMF stars and the representation in plane of the related winding configuration are used as references for the procedure validation.

4.1. 3-Phase Windings

An electrical machine composed by 24 stator slots and 2 pole pairs, equipped with a three-phase winding with $q = 2$, is used as a first validation test, which is symmetrical because $n_{wc} \in \mathbb{N}$ and $g \in \mathbb{N}$. The corresponding WDT has been already determined in Section 3.1. The data needed for the WDT construction and its related properties can be summarized as follows: $N = 24$, $m = 3$, $p = 2$, $n_{wc} = 8$,

$t = 2$, $\alpha = 30°$, $\alpha' = 30°$, $\zeta = 1$. Therefore, the corresponding WDT is composed by $m = 3$ rows and $N/m = 8$ columns, with a cell pitch equal to $p = 2$, as shown in Table 2. This winding is composed by $n_{wc} = 8$ coils per phase, which means $m \cdot n_{wc} = 3 \cdot 8 = 24$ overall coils. The EMF of each coil is represented by a phasor in the star of slots, as shown in Figure 1, which is, therefore, composed by 8 EMF phasors for each phase and by the superposition of two stars of coil EMFs ($t = 2$), where each one contains twelve phasors equally phase-shifted between each others by 30° ($\alpha' = 30°$). The EMFs corresponding to the slots 1, 2, 3, ..., 12 will have the same phase angle of the EMFs located in the slots 13, 14, 15, ..., 24, respectively. Therefore, the elements of the Table can be regrouped in 12 groups composed by $t = 2$ elements and by following the order of the Table, the linear representation of the star of slots can be detected, as it can be seen by comparing Table 2 with Figure 1.

In Table 2, the phasors (or slots) of phase 1 are written in blue color, while the phasors of phase 2 and 3 are reported in green and red colors, respectively. In order to visualize the phasors of the same phase in a single WDT row, the last 4 columns ($N/2m = 4$) of the WDT should be circularly shifted in the upper direction by a quantity equal to $\zeta = 1$ as calculated by applying (21) and that can be deduced by analyzing Table 2. The possible winding schemes that could be carried out, according to Section 3.1, are shown in Figure 2b–d.

Table 7 shows the WDT referred to a three-phase coil winding with $N = 27$, $p = 3$, for a single-layer configuration. It can be noticed that, in case of single-layer coil winding, three empty slots are required ($n_{es} = 3$) in order to satisfy the symmetry conditions. In fact

$$n_{es} = N - \frac{2 \cdot m \cdot \lfloor n_{wc} \rfloor}{n_{lay}} = 27 - \frac{2 \cdot 3 \cdot \lfloor 4.5 \rfloor}{1} = 3,$$

where

$$n_{wc} = n_{lay} \cdot \frac{N - 0}{2 \cdot m} = 1 \cdot \frac{27}{2 \cdot 3} = 4.5.$$

The corresponding unwound slots are highlighted by the crossed elements of Table 7. The winding is therefore composed by the same number of positive and negative slots. Here $Q = 1 + 1/2$ and $q = 2$. The corresponding star of slots achieved from the two WDT Table and the related winding scheme are plotted in Figure 6a,b.

Table 7. WDT for a single-layer, three-phase coil winding with $N = 27$, $m = 3$ and $p = 3$.

1	10	19	2	-11	-20	-3	-12	21̶	
4	13	22	5	-14	-23	-6	-15	24̶	$\Uparrow \zeta = 1$
7	16	25	8	-17	-26	-9	-18	27̶	

(phase 1: blue, phase 2: red, phase 3: green).

If it is necessary to fill also the empty slots only a bar winding can be here considered as shown in Figure 7a,b. In fact, only in case of single layer bar windings, n_{wc} can be a fractional number with denominator equal to 2. The corresponding WDT is reported in Table 8.

Table 8. WDT for a single-layer, three-phase bar winding with $N = 27$, $m = 3$ and $p = 3$.

1	10	19	2	11	-20	-3	-12	-21	
4	13	22	5	14	-23	-6	-15	-24	$\Uparrow \zeta = 1$
7	16	25	8	17	-26	-9	-18	-27	

(phase 1: blue, phase 2: red, phase 3: green).

As previously mentioned, the WDT can be referred to both single-layer and double-layer windings. Indeed, for double layer configurations, the position of the left side of a coil is defined by the number corresponding to the slot, whereas the position of right side is defined by the coil pitch y_c, which is

equal, in most cases, to $5/6 \cdot y_p$ (a shortened pitch employed for the limitation of both the 5-th and 7-th harmonics), where $y_p = N/2p$ is the pole pitch expressed in terms of number of slots. For instance, Table 9 shows the WDT of a double layer coil winding with $N = 27$, $p = 3$ and $q = 1 + 1/2$. Figure 8a,b refer to this double layer configuration with a coil pitch $y_c = 4$, which is composed by 3 repetitions of the basic winding with $N' = N/t' = 27/3 = 9$ slots, $m = 3$ phases and $p' = p/t' = 3/3 = 1$ pole pair. In fact

$$t' = \gcd(z, p) = \gcd(3, 3) = 3,$$

where

$$z = n_{lay} \cdot p \cdot (q - a) = 2 \cdot 3 \cdot (1.5 - 1) = 3.$$
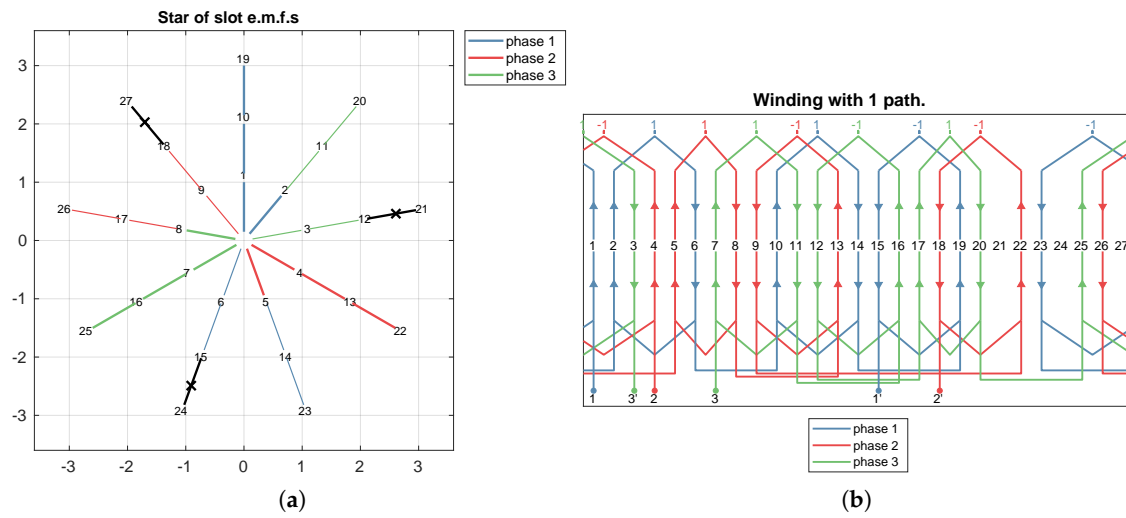
Figure 6. (**a**) Slot EMF star for a symmetrical single-layer coil winding and (**b**) winding scheme. $N = 27$, $m = 3$, $p = 3$, $Q = 1 + 1/2$ and $q = 2$.
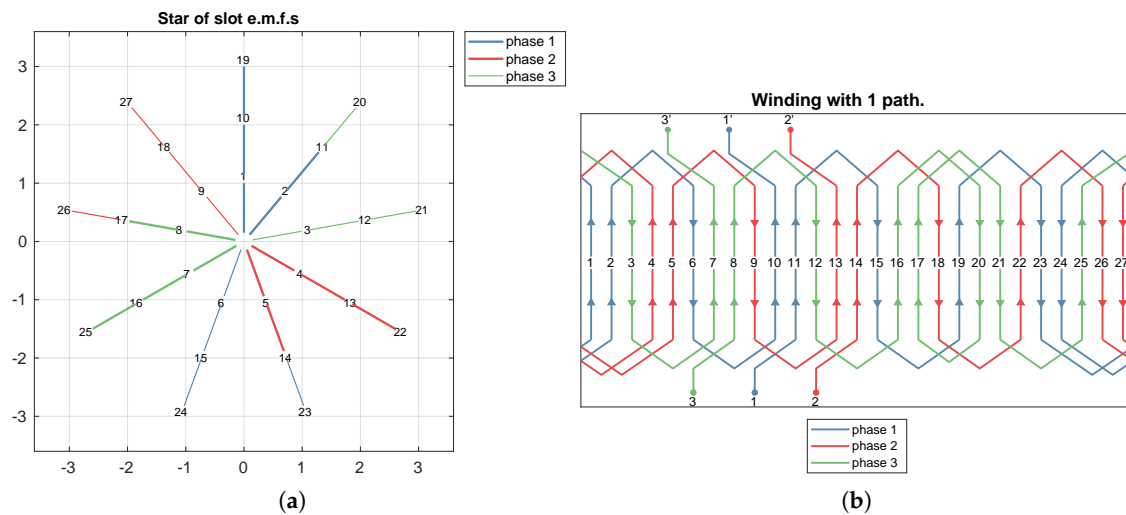
Figure 7. (**a**) Slot EMF star for a symmetrical single-layer bar winding and (**b**) winding scheme. $N = 27$, $m = 3$, $p = 3$ and $q = 1 + 1/2$.

The WDT is composed by the repetition of 3 basic WDTs: the first is created considering the slot range $1 \ldots N/t'$, the second by the slot range $N/t' + 1 \ldots 2N/t'$ and the third $2N/t' + 1 \ldots 3N/t'$. More generally, the t' slot ranges are given by $(k-1)N/t' + 1 \ldots kN/t'$ with $k = 1, \ldots, t'$. If necessary, this winding could be divided in three parallel connected paths: then, each path will be identified by the three WDTs

shown in Table 9. Figure 8b refers to a series connection of the three paths. Once the WDT is defined the right coil sides of the double layer can be added to the table. This can be made by introducing into the WDT other N/m columns as shown in Table 10, which represents the final WDT configuration. By following its rows it is possible to define the coil groups and their connections as shown in Figure 8b.

Figure 8. (**a**) Coil EMF star for a symmetrical double-layer coil winding and (**b**) winding scheme with series connected paths. $N = 27$, $m = 3$, $p = 3$, $q = 1 + 1/2$ and $y_c = 4$.
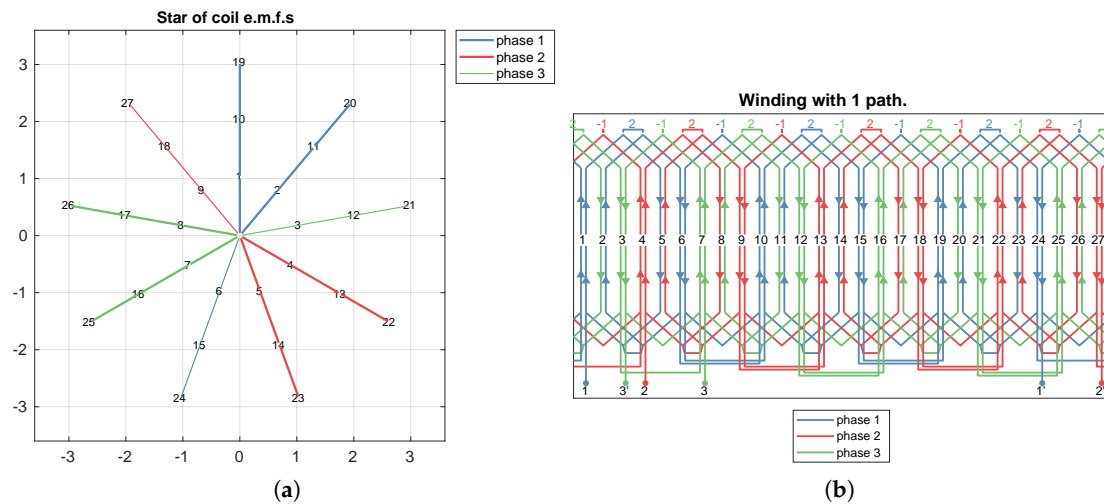
Table 9. WDT for a double-layer, three-phase winding with $N = 27$, $m = 3$ and $p = 3$.

1	2	−3		10	11	−12		19	20	−21		1	2	7	8	19	20	−3	−12	−21	
4	5	−6	+	13	14	−15	+	22	23	−24	=	4	5	13	14	22	23	−6	−15	−24	⇑ $\zeta = 1$
7	8	−9		16	17	−18		25	26	−27		7	8	16	17	25	26	−9	−18	−27	

(ph1: blue, ph2: red, ph3: green).

Table 10. WDT for a double-layer, three-phase winding with $N = 27$, $m = 3$ and $p = 3$ considering all coil sides.

1	−5	2	−6	7	−11	8	−12	19	−25	20	−24	−6	10	−15	19	−24	1
4	−8	5	−9	13	−17	14	−18	22	−26	23	−27	−9	13	−18	22	−27	4
7	−11	8	−12	16	−20	17	−21	25	−2	26	−3	−3	7	−12	16	−21	25

(ph1: blue, ph2: red, ph3: green).

The WDT method is also suitable to design fractional single and double layer concentrated windings. An example for a concentrated winding configuration is provided in Table 11, which shows the WDT related to a three-phase, double-layer non-overlapping configuration with $N = 9$, $p = 4$ and $m = 3$. The corresponding star of slots and the winding scheme are depicted in Figure 9a,b, respectively. Table 11 shows also the steps that should be followed in order to define the practical arrangement for assembling the coils in the slots: (1) the WDT is build up; (2) the negative columns are shifted upwards by ζ steps (here $\zeta = 1$); (3) the rows are ordered in ascending mode and, finally; (4) the right coil sides are introduced considering the coil span (here $y_c = 1$). Each of the m phase coils are then connected following the rows order: in this example for phase 1 coils are formed with slot pairs 8 −9, −9 1, 1 −2, for phase 2 pairs 2 −3, −3 4, 4 −5 and for phase 3 pairs 5 −6, −6 7 and 7 −8. The coils are sequentially connected as shown in Figure 9b. Therefore, WDT facilitates the selection of the optimal end-winding configuration.

Table 11. WDT for a double-layer, three-phase concentrated winding with $N = 9$ and $p = 4$.

1	8	−6		1	8	−9		8	−9	1		8	−9	−9	1	1	−2
4	2	−9	$\Longrightarrow$	4	2	−3	$\Longrightarrow$	2	−3	4	$\Longrightarrow$	2	−3	−3	4	4	−5
7	5	−3		7	5	−6		5	−6	7		5	−6	−6	7	7	−8

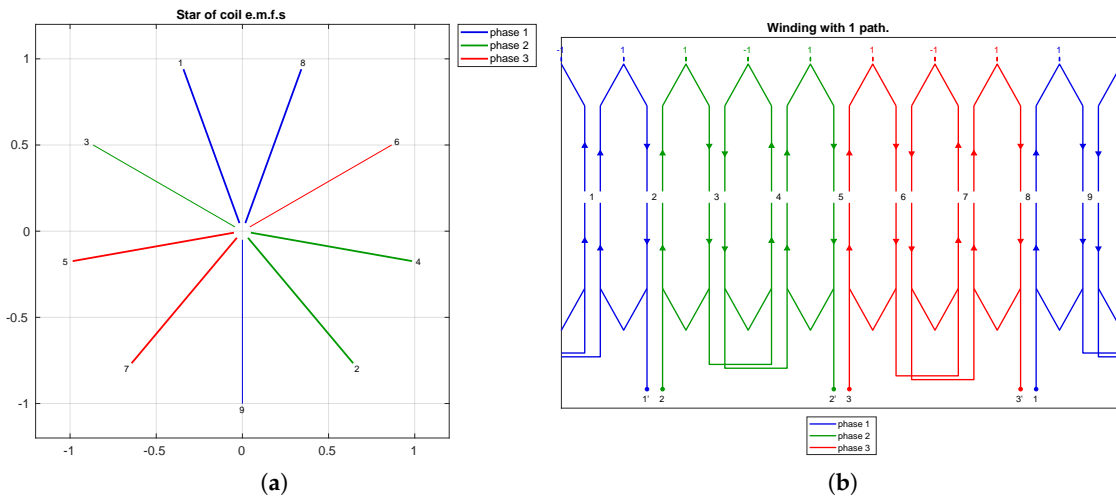(ph1: blue, ph2: green, ph3: red).

(**a**)　　　　　　　　　　(**b**)

Figure 9. (**a**) Star of slots and (**b**) winding configuration for a double-layer, three-phase concentrated winding with $N = 9$, $p = 4$ and $m = 3$.

4.2. 6-Phase Windings

An example of WDT applied to multiphase winding configurations is reported in Table 12, which shows the WDT for a six-phase, non-reduced winding with $N = 36$, $p = 5$, $n_{wc} = 3$ and $q = 3/5$, whose corresponding star of slots is shown in Figure 10a.

(**a**)　　　　　　　　　　(**b**)
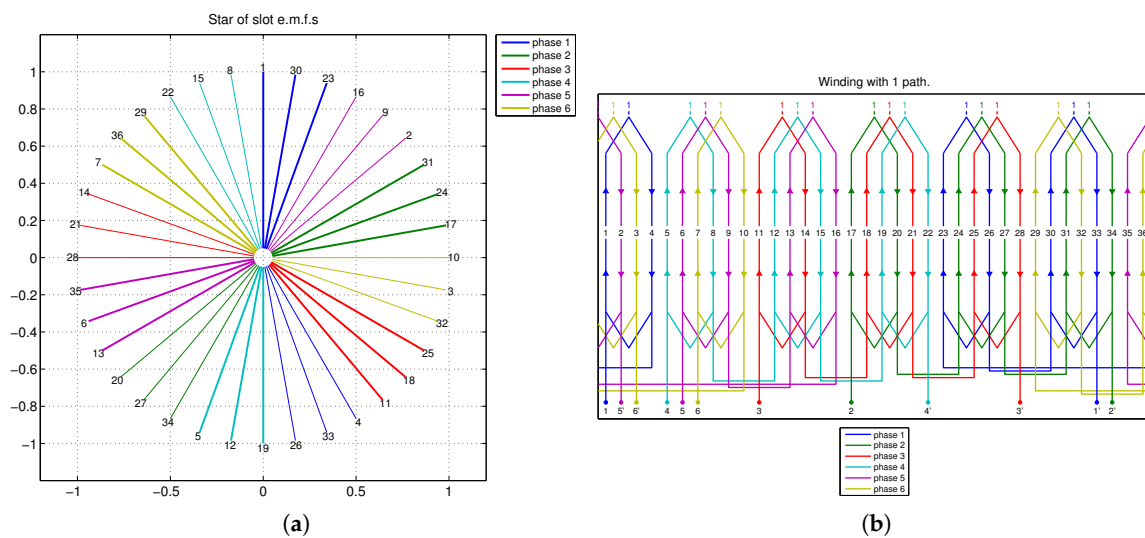
Figure 10. (**a**) EMF star and (**b**) winding scheme for a symmetrical single layer non-reduced winding with $N = 36$, $m = 6$, $p = 5$ and $q = 3/5$.

By applying now the swapping procedure to Table 12 (without shifting) and the phases reordering, following Table 6 described in Section 3.4, and by changing the sign of rows 3 and 4 in order to achieve a radial symmetry (as general rule the WDT rows of the even numbered phase groups are multiplied

by -1), it is possible to determine the WDT referred to the reduced winding configuration, shown in Table 13. The star of slots referred to this type of winding is plotted in Figure 11a. It can be noticed that this reduced configuration is composed by two groups ($m_g = 2$) of three-phase winding sections ($m_u = 3$), phase-shifted between each other by an angle corresponding to 30°: the first one is composed by phases 1–5–3, whereas the second group by phases 2–6–4.

Tables 12 and 13 can be now used to determine the winding configuration: here a single layer configuration has been chosen for the non reduced system winding, whereas a double layer one with coil pitch $y_c = 3$ has been chosen for the reduced system. The winding diagrams are shown in Figures 10 and 11b, respectively. In the case of the double layer winding, Table 13 shows only one side of the coils, i.e., the positive one, whereas the position of the other (the negative coil sides) depends on the chosen value of the coil pitch y_c.

Table 12. Winding Distribution Table for a symmetrical non-reduced winding with $N = 36$, $m = 6$, $p = 5$ and $q = 3/5$.

1	30	23	-16	-9	-2	
31	24	17	-10	-3	-32	
25	18	11	-4	-33	-26	
19	12	5	-34	-27	-20	$\Uparrow \ \zeta = 2$
13	6	35	-28	-21	-14	
7	36	29	-22	-15	-8	

(ph1: blue, ph2: green, ph3: red, ph4: cyan, ph5: magenta, ph6: yellow).

Table 13. Winding Distribution Table for a symmetrical reduced winding with $N = 36$, $m = 6$, $p = 5$ and $q = 3/5$.

1	30	23	-19	-12	-5			1	30	23	-19	-12	-5
31	24	17	-13	-6	-35			16	9	2	-34	-27	-20
25	18	11	-7	-36	-29	$\Rightarrow -1 \cdot$		-31	-24	-17	13	6	35
16	9	2	-34	-27	-20			-10	-3	-32	28	21	14
10	3	32	-28	-21	-14			25	18	11	-7	-36	-29
4	33	26	-22	-15	-8			4	33	26	-22	-15	-8

(ph1: blue, ph2: green, ph3: red, ph4: cyan, ph5: magenta, ph6: yellow).
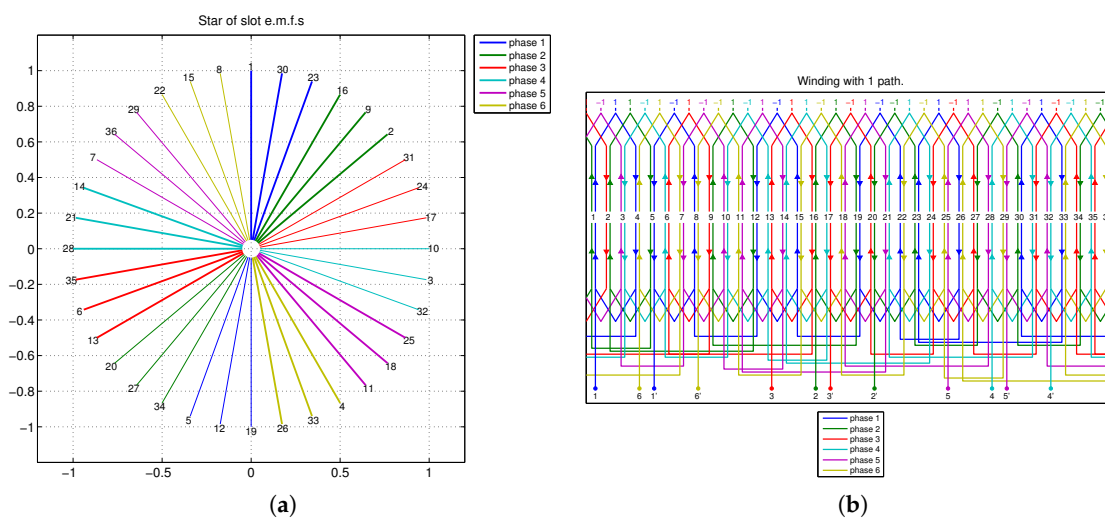

Figure 11. (**a**) EMF star and (**b**) winding scheme of a double layer reduced symmetrical configuration with $N = 36$, $m = 6$, $p = 5$ and $q = 3/5$.

4.3. 2-Phase Winding

A reduced 2-phase double-layer winding is here considered, with $N = 28$, $p = 1$, $y_c = 12$. After swapping Quadrant 1 and 3 and changing the signs of Quadrants 1 and 4 the WDT becomes as shown in Table 14. Figure 12a represents the related star of slots and Figure 12b shows the double-layer winding scheme.
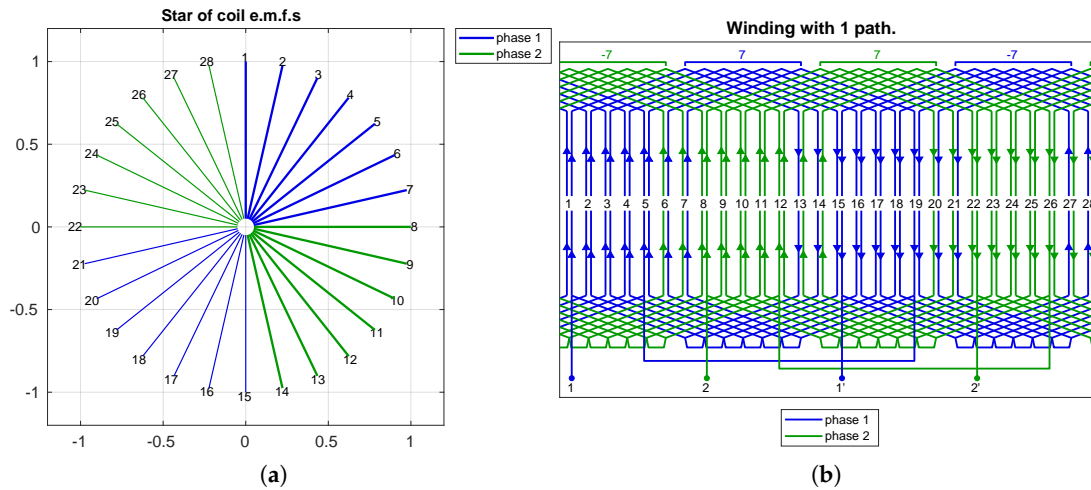

Figure 12. (**a**) Star of coils EMF and (**b**) Winding scheme for $N = 28$, $m = 2$, $p = 1$, $q = 7$ and $y_c = 12$.

Table 14. WDT for a single-layer, 2-phase winding with $N = 28$ and $p = 1$, after swapping.

1	2	3	4	5	6	7	−15	−16	−17	−18	−19	−20	−21
8	9	10	11	12	13	14	−22	−23	−24	−25	−26	−27	−28

(ph1: blue, ph2: green).

4.4. 7-Phase Winding

Another example consists in a seven-phase machine with 42 slots and 2 pole pairs. The WDT parameters can be easily determined by taking into account the equations described in Section 2. Therefore, the data needed for the WDT procedure are: $N = 42$; $m = 7$; $p = 2$; $n_{wc} = 6$; $t = 2$; $\alpha' = 17.14°$; $t' = 2$; $\zeta = 3$.

Table 15 reports the WDT for this case of study. It is a 7x6 (rows x columns) table with a cell pitch equal to 2, with six coils composing a winding phase section and two stars of 21 EMF phasors, as shown in the diagram of Figure 13a. By virtue of (11) the WDT can be divided into $t' = 2$ basic tables as shown in Table 16. The related double-layer winding scheme is depicted in Figure 13b with a chosen shortened coil pitch $y_c = 9$.

Table 15. Winding Distribution Table for a double layer winding with $N = 42$, $p = 2$ and $m = 7$.

1	2	−3		22	23	−24	1	22	2	23	−3	−24
4	5	−6		25	26	−27	4	25	5	26	−6	−27
7	8	−9		28	29	−30	7	28	8	29	−9	−30
10	11	−12	+	31	32	−33	= 10	31	11	32	−12	−33
13	14	−15		34	35	−36	13	34	14	35	−15	−36
16	17	−18		37	38	−39	16	37	17	38	−18	−39
19	20	−21		40	41	−42	19	40	20	41	−21	−42

$\Uparrow \zeta = 3$

(ph1: blue, ph2: green, ph3: red, ph4: cyan, ph5: magenta, ph6: yellow, ph7: black).

Table 16. Winding Distribution Table for a winding with $N = 72$, $p = 5$, $m = 3$ and $q = 2 + 2/5$.

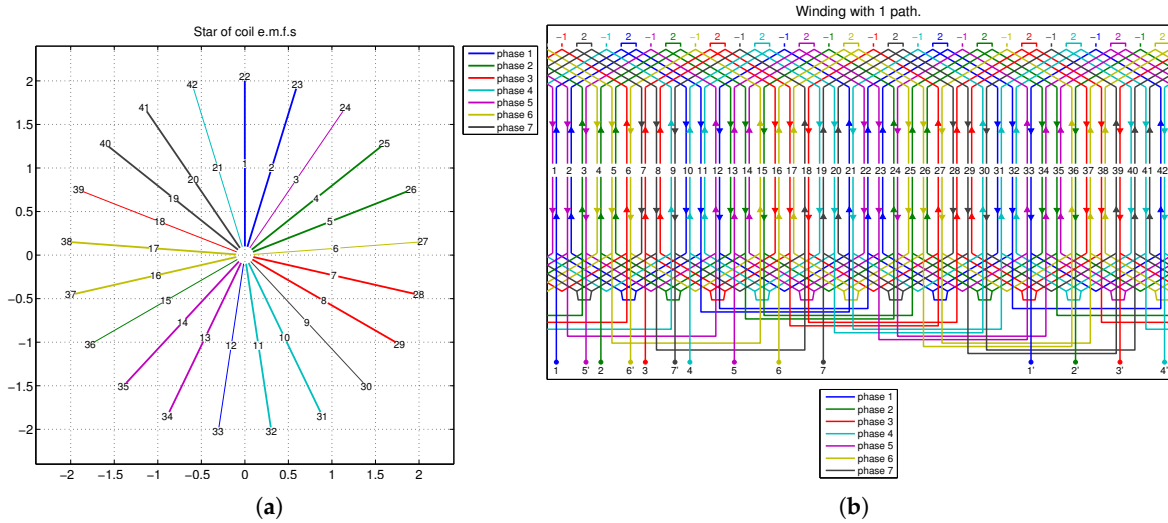| 1	30	59	16	45	2	31	60	17	46	3	32	−37	−66	−23	−52	−9	−38	−67	−24	−53	−10	−39	−68
49	6	35	64	21	50	7	36	65	22	51	8	−13	−42	−71	−28	−57	−14	−43	−72	−29	−58	−15	−44
25	54	11	40	69	26	55	12	41	70	27	56	−61	−18	−47	−4	−33	−62	−19	−48	−5	−34	−63	−20

(ph1: blue, ph2: red, ph3: green).

Figure 13. Double layer seven-phase symmetrical winding with $N = 42$, $p = 2$, $m = 7$, $y_c = 9$ and $q = 1 + 1/2$. (**a**) Star of slots and (**b**) winding scheme.

4.5. Procedures for Winding Optimization

The proposed procedure is also suitable for the implementation of winding optimization techniques, such as interspersing for single-layer windings and double chording for double layer windings. For instance, the WDT referred to a three-phase machine with $p = 5$ and a double-layer winding located into 72 slots is reported in Table 16, whereas the corresponding star of slots and winding scheme are plotted in Figure 14a,b, respectively.
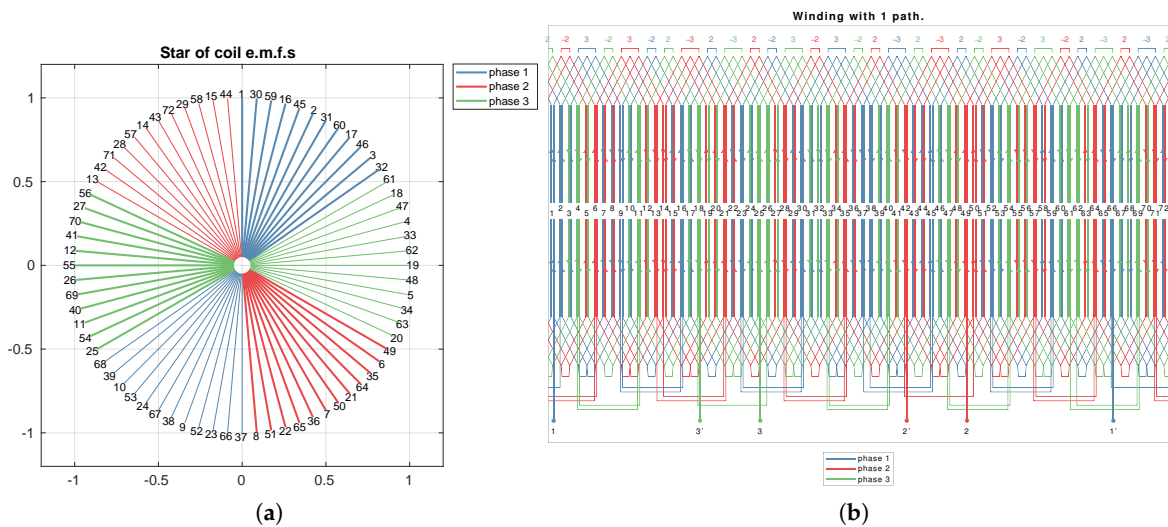

Figure 14. Three-phase symmetrical winding with $N = 72$, $p = 5$, $m = 3$ and $q = 2 + 2/5$. (**a**) Star of slots and (**b**) winding scheme.

The double chording with $y_c = 6$ and a three-order single-sided imbrication is obtained by circularly shifting upwards by two cells and by changing the sign of the first $2 \cdot j$ elements of the left side of the WDT and the first j elements of the right side of the WDT (in this case, the elements of columns nr. 2, 4 and 6 for the left side and the elements of columns nr. 13, 14 and 15 of the right are both circularly shifted and changed in sign), according to Table 17. Indeed, the corresponding star of slots is plotted in Figure 15a, whereas the modified winding scheme is plotted in Figure 15b.
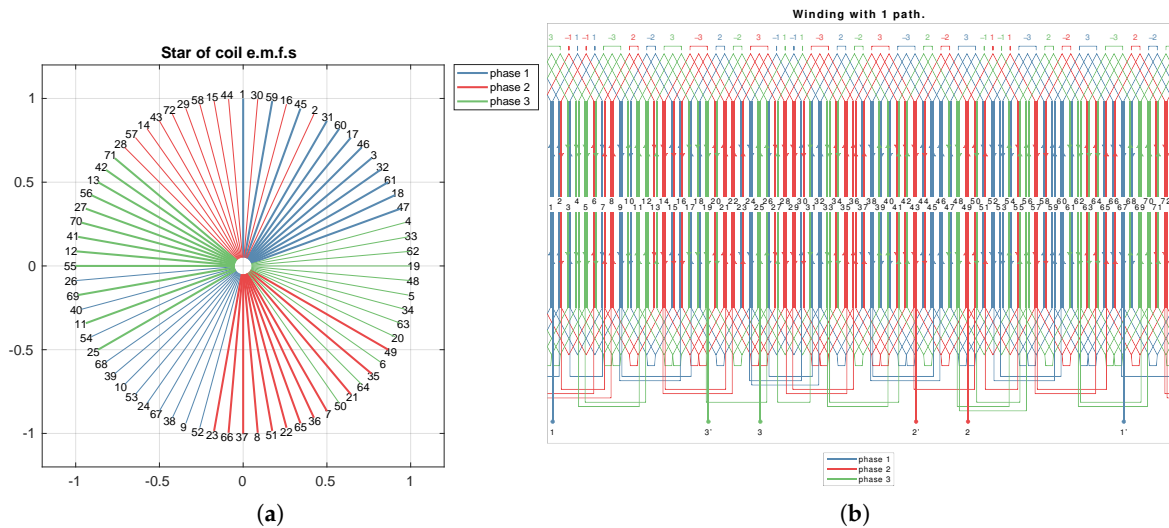

(a)   **(b)**

Figure 15. Double chording with a 3rd-order single-sided imbrication for $N = 72$, $p = 5$, $m = 3$ and $q = 2 + 2/5$. (**a**) Star of slots and (**b**) winding scheme.

Table 17. Double chording with a 3-rd order single-sided imbrication for $N = 72$, $p = 5$, $m = 3$ and $q = 2 + 2/5$.

1	−54	59	−40	45	−26	31	60	17	46	3	32	61	18	47	−52	−9	−38	−67	−24	−53	−10	−39	−68
49	−30	35	−16	21	−2	7	36	65	22	51	8	37	66	23	−28	−57	−14	−43	−72	−29	−58	−15	−44
25	−6	11	−64	69	−50	55	12	41	71	27	56	13	42	71	−4	−33	−62	−19	−48	−5	−34	−63	−20
↑		↑		↑								↑	↑	↑									

(ph1: blue, ph2: red, ph3: green).

Moreover, by shifting the WDT elements in accordance to Table 18, it is possible to implement a double chording technique with $y_c = 6$ and a double-sided imbrication with order equal to 3. This case differs from the previous one (single-sided imbrication) by the fact that the $2 \cdot j$ columns are circularly shifted for each side of the WDT, as shown by the arrows of Table 18. The corresponding star of slots and winding scheme are depicted in Figure 16a,b, respectively.

Table 18. Double chording with a 3-rd order double-sided imbrication for $N = 72$, $p = 5$, $m = 3$ and $q = 2 + 2/5$.

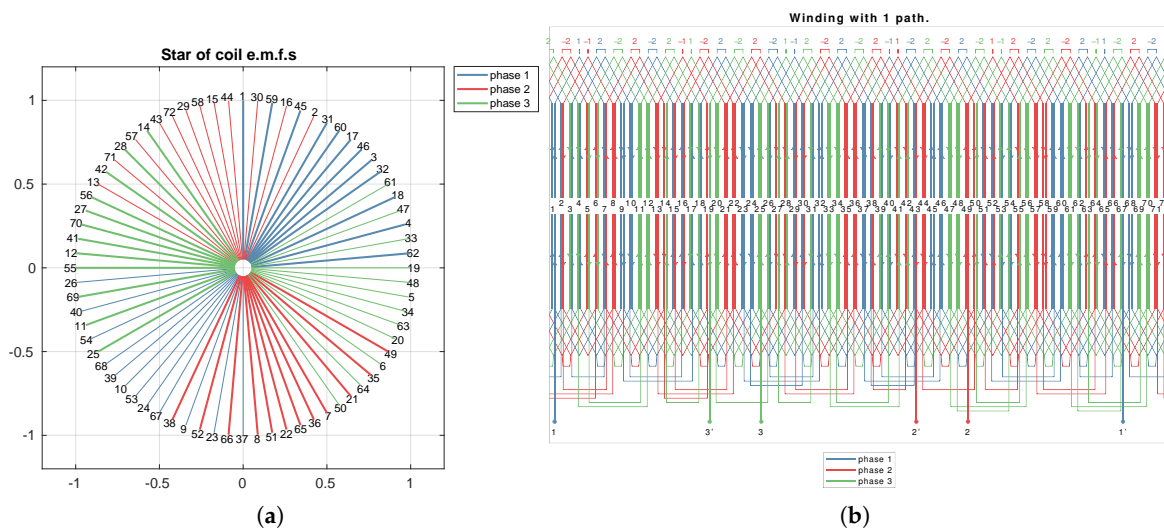| 1	−54	59	−40	45	−26	31	60	17	46	3	32	−37	18	−23	4	−9	62	−67	−24	−53	−10	−39	−68
49	−30	35	−16	21	−2	7	36	65	22	51	8	−13	66	−71	52	−57	38	−43	−72	−29	−58	−15	−44
25	−6	11	−64	69	−50	55	12	41	71	27	56	−61	42	−47	28	−33	14	−19	−48	−5	−34	−63	−20
↑		↑		↑								↑		↑		↑							

(ph1: blue, ph2: red, ph3: green).

Figure 16. Double chording with a 3rd-order double-sided imbrication for $N = 72$, $p = 5$, $m = 3$ and $q = 2 + 2/5$. (**a**) Star of slots and (**b**) winding scheme.

A triple chording can be performed in order to further reduce the winding harmonic content with the following procedures whose results are given in Table 19:

1. the WDT is developed;
2. the zone widening by two slots is performed by shifting the vertical line from the middle position to the right by two cells;
3. the double sided imbrication is made by shifting upwards by two cells the 2-nd, the 4-th and the 6-th negative columns.

Table 19. Triple chording with a 3-rd order double-sided imbrication and zone widening by 2 coils for $N = 72$, $p = 5$, $m = 3$ and $q = 2 + 2/5$.

1	−54	59	−40	45	−26	31	60	17	46	3	32	61	18	−23	4	−9	62	−67	48	−53	−10	−39	−68
49	−30	35	−16	21	−2	7	36	65	22	51	8	37	66	−71	52	−57	38	−43	24	−29	−58	−15	−44
25	−6	11	−64	69	−50	55	12	41	71	27	56	13	42	−47	28	−33	14	−19	72	−5	−34	−63	−20
↑		↑		↑										↑		↑		↑					

(ph1: blue, ph2: red, ph3: green).

Finally, Table 20 summarizes the winding factor harmonics for each of the proposed optimization technique. It can be noticed that the chording allows a significant reduction of both the fifth and the seventh order harmonics, which are almost canceled by applying a double chording technique.

Table 20. Winding factor harmonics with different optimization techniques for $N = 72$, $p = 5$, $m = 3$ and $q = 2 + 2/5$.

	Normal Chording		Double Chording		Triple Chording
Harm. Order	WDT ($y_c = 7$)	Chording ($y_c = 6$)	1-Sided Imbric.	2-Sided Imbric.	2-Sided Imbric. + Zone Widen.
1-st	0.955	0.923	0.902	0.881	0.878
3-rd	0.633	0.451	0.365	0.277	0.268
5-th	0.201	0.154	0.026	0.002	0.002
7-th	0.132	0.036	0.008	0.020	0.017
9-th	0.201	0.154	0.013	0.154	0.109
11-th	0.080	0.087	0.078	0.072	0.055

Similar results can be appreciated from the next example referred to a single-phase, double-layer winding located into 60 slots and with one pole pair. The corresponding WDT for the proposed example

is plotted in Table 21. The modified WDT for a double chording with a 2-nd order double-sided imbrication is represented in Table 22. It can be noticed that, in case of imbrication, the WDT follows the same rules of the previous example shown in Table 18 and the corresponding star of slots and winding scheme are plotted in Figure 17a,b, respectively. Table 23 summarizes the winding harmonic factors for different optimization techniques adopted for this single-phase winding.

Table 21. WDT with a double chording and a 3-rd order double-sided imbrication for $N = 60$, $p = 1$, $m = 1$ and $q = 30$.

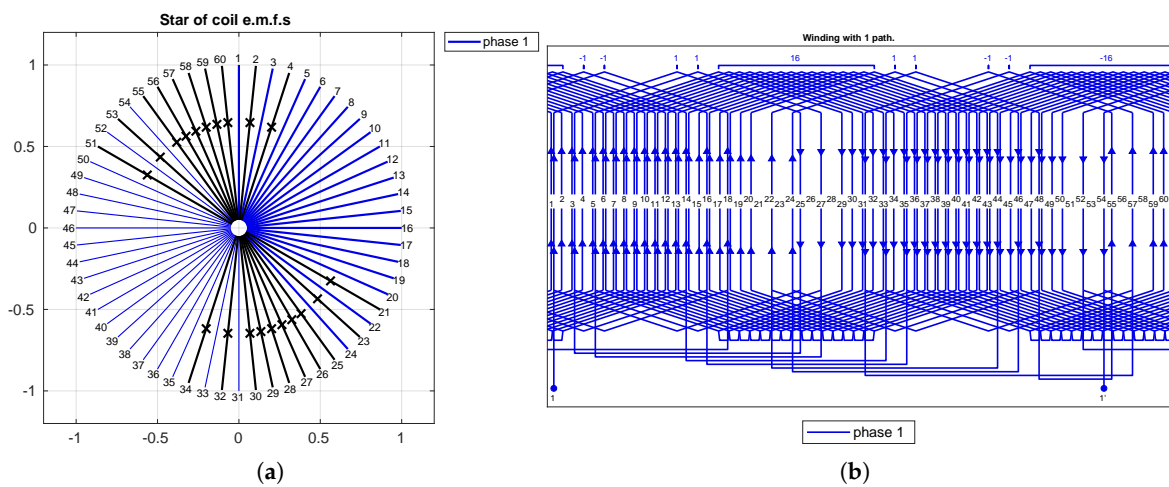| 1	2	3	4	5	6	7	8	9	10	−11	−12	−13	−14	−15	−16	−17	−18	−19	−20
21	22	23	24	25	26	27	28	29	30	−31	−32	−33	−34	−35	−36	−37	−38	−39	−40
41	42	43	44	45	46	47	48	49	50	−51	−52	−53	−54	−55	−56	−57	−58	−59	−60

Figure 17. Single phase winding with double chording, 2nd order double-sided imbrication for $N = 60$, $p = 1$, $m = 1$ and $q = 30$. (**a**) Star of slots and (**b**) winding scheme.

Table 22. WDT with a double chording and a 3-rd order double-sided imbrication for $N = 60$, $p = 1$, $m = 1$ and $q = 30$.

1	−42	3	−44	5	6	7	8	9	10	−31	12	−33	14	−35	−36	−37	−38	−39	−40
~~21~~	~~−2~~	~~23~~	~~−4~~	~~25~~	~~26~~	~~27~~	~~28~~	~~29~~	~~30~~	~~51~~	~~32~~	~~53~~	~~34~~	~~55~~	~~56~~	~~57~~	~~58~~	~~59~~	~~60~~
41	−22	43	−24	45	46	47	48	49	50	−11	52	−13	54	−15	−16	−17	−18	−19	−20
↑		↑									↑		↑						

Table 23. Winding factor harmonics with different optimization techniques for $N = 60$, $p = 1$ and $m = 1$.

Harmonic Order	WDT ($y_c = 30$)	Chording ($y_c = 24$)	Single-Sided Imbrication	Double-Sided Imbrication
1-st	0.827	0.787	0.778	0.761
3-rd	0	0	0	0
5-th	0.167	0	0	0
7-th	0.121	0.071	0.035	0.20
9-th	0	0	0	0
11-th	0.080	0.076	0.014	0.087

The imbrication procedure can now be generalized.

1.　For normal or non-reduced system windings the columns of positive slots that are to be shifted are shifted upwards by

$$s_{pos} = \begin{cases} \frac{m+1}{2} & \text{if } m \in \mathbb{U} \\ \frac{m}{2} & \text{if } m \in \mathbb{G} \end{cases} \tag{25}$$

cells, whereas the columns of negative slots must be shifted upwards by

$$s_{neg} = \begin{cases} \frac{m+1}{2} & \text{if } m \in \mathbb{U} \\ \frac{m+2}{2} & \text{if } m \in \mathbb{G} \end{cases} \tag{26}$$

2.　For reduced system windings both the positive and the negative columns are to be shifted always upwards by 1 cell, i.e.,

$$s_{pos} = 1 \text{ and } s_{neg} = 1 \tag{27}$$

The sign of the cells at the bottom of each shifted column must be then changed.

To clarify the procedure to carry out an imbrication in a reduced winding the following example is presented. Here a 6-phase reduced winding with $N = 96$, $p = 5$, $q = 1 + 2/10$ is considered.

After swapping Quadrants 1 and 3 of Table 24 and reordering it following Table 6 we obtain Table 25.

Table 24. WDT of a 6-phase reduced winding with $N = 96$, $p = 5$, $q = 1 + 2/10$.

1	30	59	16	45	2	31	60	17	46	3	32
61	18	47	4	33	62	19	48	5	34	63	20
49	6	35	64	21	50	7	36	65	22	51	8
37	66	23	52	9	38	67	24	53	10	39	68
25	54	11	40	69	26	55	12	41	70	27	56
13	42	71	28	57	14	43	72	29	58	15	44

Table 25. WDT of a 6-phase reduced winding with $N = 96$, $p = 5$, $q = 1 + 2/10$, after swapping.

1	30	59	16	45	2	−37	−66	−23	−52	−9	−38
31	60	17	46	3	32	−67	−24	−53	−10	−39	−68
61	18	47	4	33	62	−25	−54	−11	−40	−69	−26
19	48	5	34	63	20	−55	−12	−41	−70	−27	−56
49	6	35	64	21	50	−13	−42	−71	−28	−57	−14
7	36	65	22	51	8	−43	−72	−29	−58	−15	−44
	↑						↑				

(ph1: blue, ph2: green, ph3: red, ph4: cyan, ph5: magenta, ph6: yellow).

Now, by shifting upwards both columns 2 and 8 by one cell ($s_{pos} = 1$ and $s_{neg} = 1$), and by changing the signs of the cells in the last row of the shifted columns (here row nr. 6) we obtain, finally, Table 26. Here again, in order to realize a radial symmetrical system, the even phase groups must be multiplied by -1 (i.e., rows 3 and 4 in Table 26).

Table 26. WDT of a 6-phase reduced winding with $N = 96$, $p = 5$, $q = 1 + 2/10$, and double sided imbrication of the 1-st order.

	1	60	59	16	45	2	−37	−24	−23	−52	−9	−38
	31	18	17	46	3	32	−67	−54	−53	−10	−39	−68
$-1 \cdot$ {	61	48	47	4	33	62	−25	−12	−11	−40	−69	−26
	19	6	5	34	63	20	−55	−42	−41	−70	−27	−56
	49	36	35	64	21	50	−13	−72	−71	−28	−57	−14
	7	−30	65	22	51	8	−43	66	−29	−58	−15	−44

(ph1: blue, ph2: green, ph3: red, ph4: cyan, ph5: magenta, ph6: yellow).

The star of slots of the final winding configuration with imbrication is shown in Figure 18a, whereas the related final scheme is shown in Figure 18a.
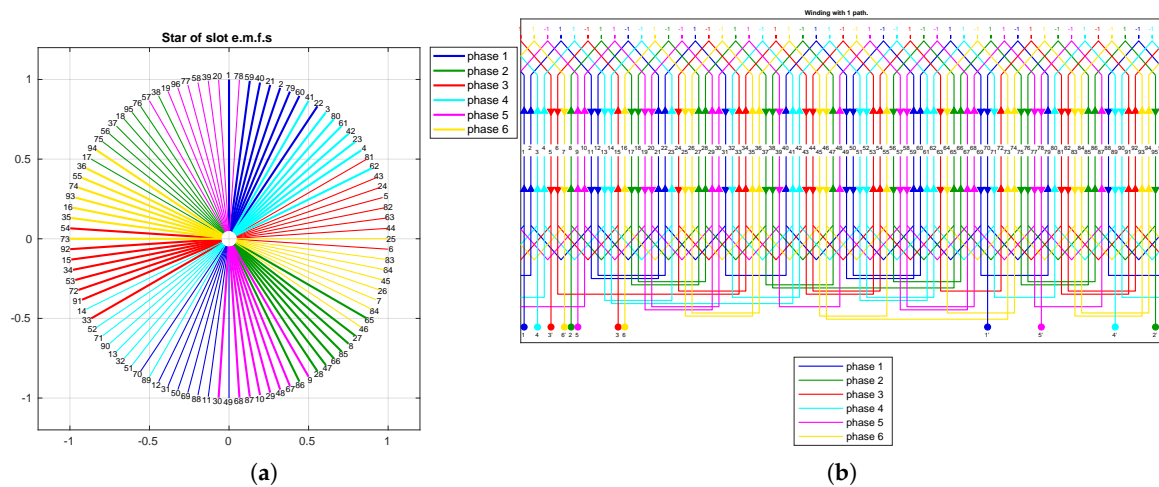

Figure 18. (**a**) Star of slots of a 6-phase reduced single-layer winding with $N = 96$, $p = 5$ and (**b**) related winding scheme with 1-st order double sided imbrication.

5. Conclusions

In this paper a new, simple and effective procedure for the determination of the EMF stars distribution and the winding configuration in all possible typologies of electrical machines equipped with symmetrical windings by means of the WDT has been presented. The main advantage of the WDT consists in its very simple construction and interpretation, which simplifies also the determination of the winding characteristics in terms of harmonic content and end-winding configuration. With this method the construction of stars of slots is no longer needed, even if in this paper they have been shown but only for clarity's sake. Furthermore, as reported in the various examples, WDT can be applied to all type of windings, allowing the resolution of complex problems by adopting only 3 fundamental rules. Winding optimization procedures, such as double chording, interspersing (single or double-sided) and zone widening or shortening can be easily implemented with simple and general standard procedures and can be applied to all type of windings derived by both reduced and normal systems. Moreover, the WDT is easy to be implemented on a computer and it can, therefore, be considered as a very useful tool particularly within the phase of rapid winding design. The winding examples proposed in this work include symmetrical windings with integer and fractional slot numbers both normal and reduced (radial symmetrical windings). The examples shown successfully validate the WDT procedure.

Author Contributions: Authors contributed equally to this work. Authors of this manuscript jointly conceived theoretical developments, revised the state of the art, provided suggestions for testing the method on windings with different slots/pole combinations.

Conflicts of Interest: The authors declare no conflict of interest.

Nomenclature

N nr. of slots;
m nr. of phases;
p nr. of pole pairs;
n_{wc} nr. of wound coils per phase;
n_{lay} nr. of winding layers;

n_{es}　　nr. of empty slots;
Q　　　nr. of slots per pole per phase;
q　　　nr. of wound slots per pole per phase;
t　　　greatest common divider between N and p;
y_c　　coil pitch (or coil span);
$\mathbb{N}$　　the set of natural numbers;
$\mathbb{G}$　　the set of even numbers;
$\mathbb{U}$　　the set of odd numbers.

Appendix

The Matlab® code for populating WDT is here reported.

```
M=zeros(1,N);
i=1;
while i<=N
    ind=mod(p*(i-1)+1,N);
    if ind==0
        ind=N;
    end
    while M(ind)~=0
        ind=ind+1;
    end
    M(ind)=i;
    i=i+1;
    ind=ind+1;
end
display(M);
M1=zeros(m,2/n_lay*n_wc);
for i=1:m
    M1(i,:)=M(2/n_lay*n_wc*(i-1)+1:2/n_lay*n_wc*i);
end
```

References

1.　Arnold, E. *Die Ankerwicklungen und Ankerkonstruktionen der Gleichstrom-Dynamomaschinen*, 3rd ed.; Springer: Berlin/München, Germany, 1899.
2.　Arnold, E. *Die Wicklungen der Wechselstrommaschinen*, 2nd ed.; Die Wechselstromtechnik; Verlag von Julius Springer: Berlin, Germany, 1912; Volume 3.
3.　Richter, R. *Ankerwicklungen für Gleich- und Wechselstrommaschinen: Ein Lehrbuch*; Springer Verlag: Berlin, Germany, 1920.
4.　Kauders, W. Systematik der Drehstromwicklungen. II. Teil. *Elektrotechnik und Maschinenbau* **1934**, *52*, 85.
5.　Heller, F.; Kauders, W. Das Görgessche Durchflutungspolygon. *Arch. Elektrotech.* **1935**, *29*, 599–616.
6.　Richter, R. *Lehrbuch der Wicklungen elektrischer Maschinen*; Wissenschaftliche Bücherei; Verlag und Druck G. Braun: Karlsruhe, Germany, 1952.
7.　Sequenz, H. *Die Wicklungen elektrischer Maschinen: Wechselstrom Ankerwicklungen.*; Springer Verlag: Wien, Austria, 1950; Volume 1.
8.　Sequenz, H. *Die Wicklungen Elektrischer Maschinen: Wenderwicklungen*; Springer Verlag: Wien, Austria, 1952; Voluem 2.
9.　Sequenz, H. *Die Wicklungen Elektrischer Maschinen: Wechselstrom-Sonderwicklungen*; Springer Verlag: Wien, Austria, 1954; Volume 3.
10.　De Pistoye, H. Bobinages à courant alternatif à trous partiels. *Revue Générale de l'Electricité* **1923**, *14*, 798.
11.　Heller, B.; Hamata, V. *Harmonic Field Effects in Induction Machines*; Elsevier Scientific Pub. Co.: Amsterdam, The Netherlands, 1977.

12. Rebora, G. Avvolgimenti trifase. *Elettrotecnica* **1931**, *618*, 72.

13. Seike, T. Die einfache Ausführung der Bruchloch-Ankerwicklungen für Wechselstrom. *Elektrotech. Masch.* **1931**, *49*, 21.

14. Liwschitz-Garik, M.; Gentilini, C. *Winding Alternating-Current Machines: A Book for Winders, Repairmen, and Designers of Electric Machines*; Van Nostrand: New York, NY, USA, 1950.

15. Liwschitz, M.M. Balanced fractional-slot wave windings. *Electr. Eng.* **1948**, *67*, 893–893.

16. Liwschitz, M.M. Doubly chorded fractional-slot windings. *Electr. Eng.* **1948**, *67*, 848–848.

17. Malti, M.G.; Herzog, F. Fractional-slot and dead-coil windings. *Electr. Eng.* **1940**, *59*, 782–794.

18. Hellmund, R.; Veinott, C. Irregular windings in wound rotor induction motors. *Electr. Eng.* **1934**, *53*, 342–346.

19. Tingley, E.M. Two- and Three-Phase Lap Windings in unequal Groups. *Electr. Rev. West. Electr.* **1915**, *66*, 166–168.

20. Di Tommaso, A.O.; Genduso, F.; Miceli, R. A New Software Tool for Design, Optimization, and Complete Analysis of Rotating Electrical Machines Windings. *IEEE Trans. Magnet.* **2015**, *51*, 1–10.

21. Smith, A.; Delgado, D. Automated AC Winding Design. In Proceedings of the 5th IET International Conference on Power Electronics, Machines and Drives (PEMD 2010), Brighton, UK, 19–21 April 2010; pp. 1–6.

22. Steinbrink, J. Design and Analysis of Windings of Electrical Machines. In Proceedings of the International Symposium on Power Electronics, Electrical Drives, Automation and Motion (SPEEDAM 2008), Ischia, Italy, 11–13 June 2008; pp. 717–720.

23. Bianchi, N.; Pre, M.D. Use of the star of slots in designing fractional-slot single-layer synchronous motors. *IEE Proc.* **2006**, *153*, 459–466.

24. Wach, P. Algorithmic method of design and analysis of fractional-slot windings of AC machines. *Electr. Eng.* **1998**, *81*, 163–170.

25. Huth, G. Optimierung des Wicklungssystems bei permanentmagneterregten AC-Servomotoren. *Electr. Eng.* **1999**, *8*, 375–383.

26. Di Tommaso, A.O.; Genduso, F.; Miceli, R.; Galluzzo, G.R. An Exact Method for the Determination of Differential Leakage Factors in Electrical Machines With Non-Symmetrical Windings. *IEEE Trans. Magnet.* **2016**, *52*, 1–9.

27. Germishuizen, J.J.; Kamper, M.J. Classification of symmetrical non-overlapping three-phase windings. In Proceedings of the XIX International Conference on Electrical Machines—ICEM 2010, Rome, Italy, 6–8 September 2010; pp. 1–6.

28. Bianchi, N.; Prè, M.; Alberti, L. *Theory and Design of Fractional-Slot Pm Machines*; IEEE IAS Tutorial Course Notes; CLEUP: Padova, Italy, 2007.

29. Alberti, L.; Bianchi, N. Theory and Design of Fractional-Slot Multilayer Windings. *IEEE Trans. Ind. Appl.* **2013**, *49*, 841–849.

30. Abdennadher, I.; Masmoudi, A. Star of slots-based graphical assessment of the back-EMF of fractional-slot PM synchronous machines. In Proceedings of the 10th International Multi-Conferences on Systems, Signals Devices 2013 (SSD13), Hammamet, Tunisia, 18–21 March 2013; pp. 1–8.

31. Ugalde, G.; Poza, J.; Rodriguez, M.A.; Gonzalez, A. Space harmonic modeling of fractional permanent magnet machines from star of slots. In Proceedings of the 2008 18th International Conference on Electrical Machines, Vilamoura, Portugal, 6–9 September 2008; pp. 1–6.

32. Wach, P. Multi-phase systems of fractional-slot windings of AC electrical machines. *Arch. Electr. Eng.* **1997**, *46*, 471–486.

33. Pyrhonen, J.; Jokinen, T.; Hrabovcová, V. *Design of Rotating Electrical Machines*, 2nd ed.; John Wiley & Sons: New Delhi, India, 2014.

34. Heiles, F. *Wicklungen Elektrischer Maschinen und ihre Herstellung*, 2nd ed.; Springer: Berlin/Göttingen/Heidelberg, Germany, 1953; p. 270.

35. Müller, G.; Vogt, K.; Ponick, B. *Berechnung Elektrischer Maschinen*, 6th ed.; Elektrische Maschinen; Wiley-VCH Verlag GmbH & Co KGaA: Weinheim, Germany, 2008.

36. Huth, G. Eigenschaften strangverschachtelter Einschichtwicklungen für Drehstrom-Asynchronmotoren. *Electr. Eng.* **1997**, *80*, 369–373.